

Interferometry-aided terahertz time-domain spectroscopy

DANIEL MOLTER,^{1,*} MANUEL TRIERWEILER,¹ FRANK ELLRICH,¹
JOACHIM JONUSCHEIT,¹ AND GEORG VON FREYMAN^{1,2}

¹Fraunhofer Institute for Industrial Mathematics ITWM, 67663 Kaiserslautern, Germany

²Department of Physics and Research Center OPTIMAS, University of Kaiserslautern,
67663 Kaiserslautern, Germany

*daniel.molter@itwm.fraunhofer.de

Abstract: Terahertz time-domain spectroscopy as well as all optical pump-probe techniques with ultrashort pulses relies on the exact knowledge of an optical delay between related laser pulses. Classical realizations of the measurement principle vary the optical path length for one of the pulses by mechanical translation of optical components. Most commonly, only an indirect measurement of the translation is carried out, which introduces inaccuracies due to imprecise mechanics or harsh environment. We present a comprehensive study on the effect of delay inaccuracies on the quality of terahertz spectra acquired with time-domain spectroscopy systems and present an interferometric technique to directly acquire the optical delay simultaneously to the terahertz measurement data. This measurement principle enables high-precision terahertz spectroscopy even in harsh environment with non-systematic disruptions.

© 2017 Optical Society of America

OCIS codes: (300.6495) Spectroscopy, terahertz; (120.3180) Interferometry; (120.3940) Metrology.

References and links

1. H. Merbold, D. J. H. C. Maas, and J. L. M. van Mechelen, "Multiparameter sensing of paper sheets using terahertz time-domain spectroscopy: Caliper, fiber orientation, moisture, and the role of spatial inhomogeneity," in *SENSORS, 2016 IEEE* (IEEE, 2016) pp. 1–3.
2. S. Krimi, J. Klier, J. Jonuscheit, G. von Freymann, R. Urbansky, and R. Beigang, "Highly accurate thickness measurement of multi-layered automotive paints using terahertz technology," *Appl. Phys. Lett.* **109**, 021105 (2016).
3. T. Yasui, T. Yasuda, K.-i. Sawanaka, and T. Araki, "Terahertz paintmeter for noncontact monitoring of thickness and drying progress in paint film," *Appl. Opt.* **44**, 6849–6856 (2005).
4. Ch. Fattinger and D. Grischkowsky, "Terahertz beams," *Appl. Phys. Lett.* **54**(6), 490–492 (1989).
5. D. Grischkowsky, S. Keiding, M. van Exter, and Ch. Fattinger, "Far-infrared time-domain spectroscopy with terahertz beams of dielectrics and semiconductors," *J. Opt. Soc. Am. B* **7**, 2006–2015 (1990).
6. Y. Wang, C. Wang, Q. Xing, F. Liu, Y. Li, L. Chai, Q. Wang, F. Fang, and X. Zhang, "Periodic optical delay line based on a tilted parabolic generatrix helicoid reflective mirror," *Appl. Opt.* **48**, 1998–2005 (2009).
7. D. Molter, F. Ellrich, T. Weinland, S. George, M. Goiran, F. Keilmann, R. Beigang, and J. Léotin, "High-speed terahertz time-domain spectroscopy of cyclotron resonance in pulsed magnetic field," *Opt. Express* **18** 26163–26168 (2010).
8. B. Reitemeier, S. F. Busch, T. Probst, M. Scheller, and M. Koch, "Low-cost delay line for fast terahertz imaging," in *Infrared, Millimeter, and Terahertz Waves (IRMMW-THz), 2013 38th International Conference on* (IEEE, 2013).
9. F. Ellrich, T. Weinland, D. Molter, J. Jonuscheit, and R. Beigang, "Compact fiber-coupled terahertz spectroscopy system pumped at 800 nm wavelength," *Rev. Sci. Instrum.* **82**, 053102 (2011).
10. W. Withayachumnankul, B. M. Fischer, H. Lin, and D. Abbott, "Uncertainty in terahertz time-domain spectroscopy measurement," *J. Opt. Soc. Am. B* **25**(6), 1059–1072 (2008).
11. A. Soltani, T. Probst, S. F. Busch, M. Schwerdtfeger, E. Castro-Camus, and M. Koch, "Error from delay drift in terahertz attenuated total reflection spectroscopy," *J. Infrared, Millimeter, Terahertz Waves* **35**(5), 468–477 (2014).
12. W. Withayachumnankul and M. Naftaly, "Fundamentals of measurement in terahertz time-domain spectroscopy," *J. Infrared Millimeter Terahertz Waves* **35**(8), 610–637 (2014).
13. D. Jahn, S. Lippert, M. Bisi, L. Oberto, J. C. Balzer, and M. Koch, "On the Influence of Delay Line Uncertainty in THz Time-Domain Spectroscopy," *J. Infrared Millimeter Terahertz Waves* **37**(6), 605–613 (2016).
14. A. Rehn, D. Jahn, J. C. Balzer, and M. Koch, "Periodic Sampling Errors in THz Measurements," in *Infrared, Millimeter, and Terahertz waves (IRMMW-THz), 2016 41st International Conference on* (IEEE, 2016).
15. M. van Exter, Ch. Fattinger, and D. Grischkowsky, "Terahertz time-domain spectroscopy of water vapor," *Opt. Lett.* **14**(20), 1128–1130 (1989).

16. L.S. Rothman, I.E. Gordon, Y. Babikov, A. Barbe, D. Chris Benner, P.F. Bernath, M. Birk, L. Bizzocchi, V. Boudon, L.R. Brown, A. Campargue, K. Chance, E.A. Cohen, L.H. Coudert, V.M. Devi, B.J. Drouin, A. Fayt, J.-M. Flaud, R.R. Gamache, J.J. Harrison, J.-M. Hartmann, C. Hill, J.T. Hodges, D. Jacquemart, A. Jolly, J. Lamouroux, R.J. Le Roy, G.Li, D.A. Long, O.M. Lyulin, C.J. Mackie, S.T. Massie, S. Mikhailenko, H.S.P. Müller, O.V. Naumenko, A.V. Nikitin, J. Orphal, V. Perevalov, A. Perrin, E.R. Polovtseva, C. Richard, M.A.H. Smith, E. Starikova, K. Sung, S. Tashkun, J. Tennyson, G.C. Toon, V.I.G. Tyuterev, and G. Wagner, "The HITRAN2012 molecular spectroscopic database," *J. Quantitative Spectroscopy Radiative Transfer* **130**, 4–50 (2013).
17. M. Herrmann, F. Platte, K. Nalpanitidis, R. Beigang, and H. M. Heise, "Combination of Kramers-Kronig transform and time-domain methods for the determination of optical constants in THz spectroscopy," *Vibrational Spectroscopy* **60** 107–112 (2012).
18. V. Greco, G. Molesini, and F. Quercioli, "Accurate polarization interferometer," *Rev. Sci. Instrum.* **66**(7), 3729–3734 (1995).
19. J. D. Ellis, *Field Guide to Displacement Measuring Interferometry* (SPIE, 2014).

1. Introduction

As real-world applications of terahertz technology are becoming more and more realistic [1–3], the demands on measurement devices in terms of stability and robustness are rising. The employment of these systems in harsh industrial environments is challenging in particular for time-domain spectroscopy systems. The measurement principle of these systems [4,5] relies on the exact timing of two optical branches, which are fed with femtosecond pulses realizing the sampling method. Although complex delay-line concepts have been reported in the past [6–9], the timing variation is mostly realized by introducing mechanically movable optical components like mirrors or retroreflectors. The effort to increase the timing accuracy by employing very precise mechanical and electronic components only partially alleviates the problem. Moreover, these high-end products increase the system price inevitably, which impedes the application of these systems to real-world industrial tasks. Furthermore, any influence on the timing due to external factors has impact on the measurement quality and has been investigated in detail by many groups [10–14].

Instead of improving the component's accuracy, we realize the improvement of measurement quality by simultaneously measuring the inaccuracy and deviation from the perfect desired timing and taking into account these deviations in time-information on the analysis of raw terahertz time-domain data. The measurement of component translation is accomplished by implementing a coaxial interferometer into the delay-line section of the time-domain spectroscopy system. With this principle, it is possible to achieve very precise results even by using mechanically most inaccurate and highly cost-efficient translation components, e.g. servo motors from the RC model market.

2. Simulation

To fully understand the influence of delay-line uncertainties on terahertz spectra from time-domain systems, numerical simulations are carried out. The best indicators for the quality of terahertz spectra are the positions and line shapes of water vapor absorptions in ambient air, due to the fact, that they are present in most of the terahertz spectra of real-world applications and are therefore well-known to the community [15]. Furthermore, the HITRAN database [16] provides accurate parameters to calculate the absorption spectra of water vapor at various ambient conditions. For this reason, we focus in this paper on the influence of delay uncertainties on the absorption spectra of moist air. A scheme of our simulation principle is sketched in Fig. 1. As the source of the timing deviation is obviously located in the time domain, we have to transfer the frequency-domain data from HITRAN to the time domain. To do so, we first calculate the absorption spectrum for a given setup and take into account the terahertz optical path length, the relative humidity, the pressure and the temperature. By applying Kramers-Kronig relations [17], we calculate the complex index of refraction, which is needed to determine the influence of

absorption on amplitude and phase of a terahertz spectrum. This terahertz spectrum of an ideal terahertz pulse is derived via fast Fourier transform of a calculated terahertz pulse. The terahertz pulse is numerically generated with a simple model taking into account the laser pulse duration and charge carrier lifetime in the semiconductor of the photoconductive switch. Once the terahertz spectrum contains the information of the water vapor absorption, an inverse fast Fourier transform leads to the terahertz pulse in the time domain with the characteristic echoes after the main pulse originating from the water vapor absorption lines. This time-domain data is the base for further investigation, representing a perfect measurement result based on a perfectly linear time base. This linear time base is then distorted by addition of a characteristic delay error. After distortion, the amplitude information is mapped onto a linear time base by linear interpolation, resulting in a distorted time-domain pulse. Applying fast Fourier transform finally reveals the influence on the terahertz spectrum.

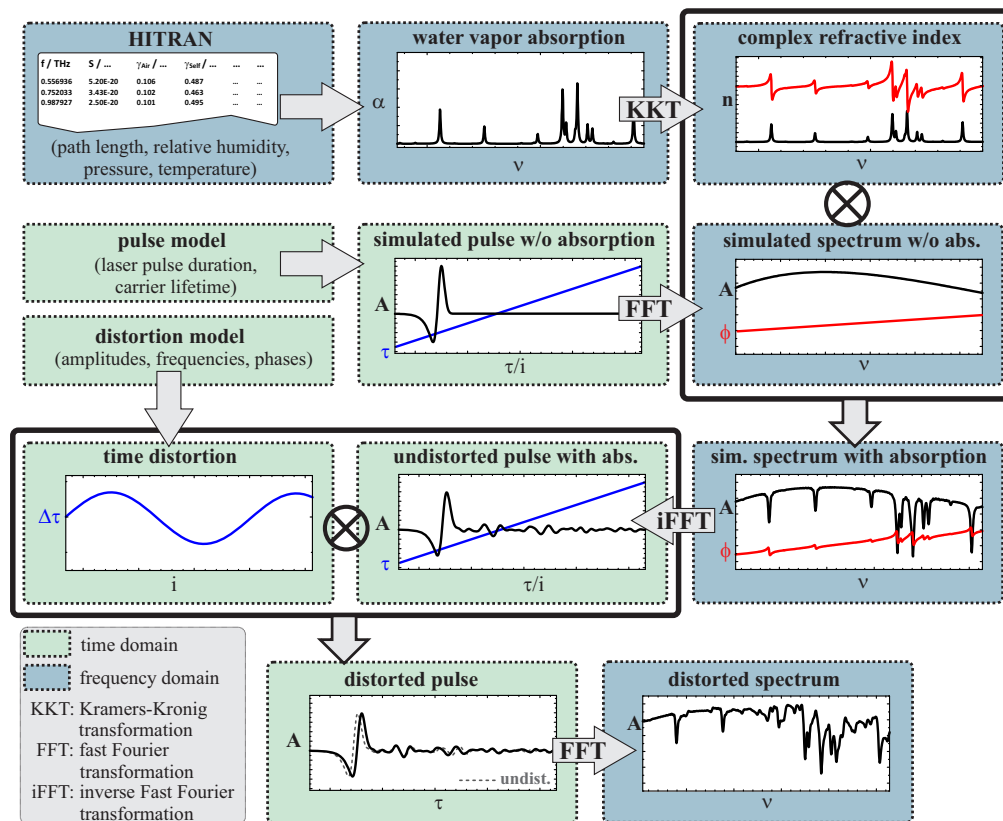


Fig. 1. Scheme of the simulation to determine the effect of delay distortion on terahertz time-domain spectra. Starting from HITRAN data, a water vapor absorption spectrum is calculated taking into account the optical path length, temperature, relative humidity, pressure and partial gas pressure. Kramers-Kronig transformations are used to calculate the complex refractive index. The information of the complex index of refraction is added to the simulated spectrum without absorption features (obtained from a pulse model in the time-domain and following Fourier transformation) to retrieve a perfect spectrum with water vapor absorption lines. Subsequent inverse fast Fourier transformation provides the undistorted pulse with absorption features. Its linear time base is superimposed with a distortion and the resulting distorted pulse is transferred to the frequency domain by fast Fourier transform.

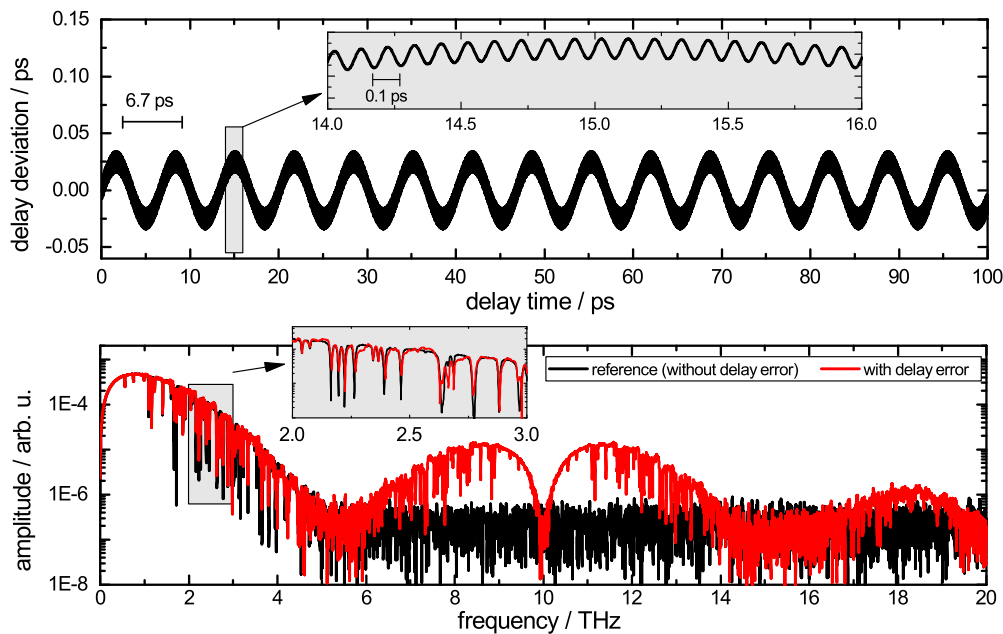


Fig. 2. Simulation result of a high frequency delay deviation typical for motor-driven linear axes. The upper part of this figure shows the assumed deviation, which consists of two frequency components (periodicities of 6.7 ps and 0.1 ps). The lower part shows the influence of this deviation on the terahertz spectrum. Besides the asymmetry of the water vapor absorption lines, a very prominent ghost spectrum around 10 THz appears, whose location is related to the periodicity in the time domain.

Based on this simulation procedure, the influence of different delay deviations can be investigated. The type of delay deviation is determined by the assumed delay unit. Delay lines based on motor-driven linear stages typically show deviations with a periodicity related to the drive (leadscrew or circulating ballscrew). Common pitches are in the range of 1 mm per revolution, which results in a periodicity in time domain of about 6.7 ps, when assuming a classical single-pass delay line. In our considerations, we assume a deviation consisting of multiple components. In Fig. 2, two components are considered with 6.7 ps and 0.1 ps periodicity, respectively. The influence of this delay deviation on the terahertz spectrum is shown in the lower plot. The periodicity of 6.7 ps leads to line shape deviations in the terahertz spectrum, whereas the 0.1 ps component leads to the formation of a symmetric ghost spectrum around 10 THz. The time step and span of the data in the simulation was 0.025 ps and 100 ps, respectively.

Voice-coil driven delay units most commonly show a fundamentally different deviation, as they base on oscillating components. Therefore, the systematic delay deviation is a superposition of the fundamental and higher harmonics of the oscillation frequency, but can vary in phase, depending on the individual device, fundamental oscillation frequency and amplitude. Fig. 3 shows three examples of the simulated influence of typical delay deviations of a voice-coil driven delay unit. The periodic delay deviation assumed in this case is a sum of the first three harmonics of the fundamental frequency and varies in amplitude and phase. Depending on these factors, the influence on the absorption features is different. The amplitude in general defines the shift in frequency, whereas the phase determines the direction of this shift and the asymmetry of the line shape. The impact of this delay deviation is higher at higher terahertz frequencies, emphasizing the need for a solution of this problem, as the accessible and usable frequency range increases in recent time-domain spectroscopy systems.

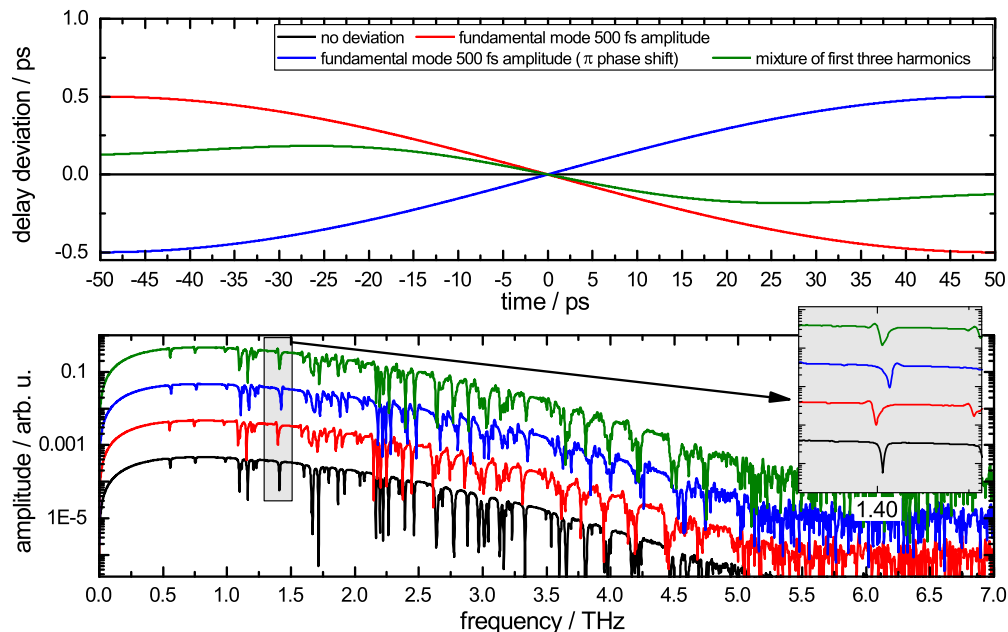


Fig. 3. Simulation results of low frequency delay deviations typical for voice-coil driven delay units. Different amplitudes lead to different shifts, whereas the phase of the deviation determines the direction of frequency shift and asymmetry. The spectra are vertically shifted for clarity.

With these simulation results, observed experimental results can be fundamentally interpreted and sources of measurement imperfections can be determined more precisely. The final aim of our approach is not only to understand the influence of this delay deviations, but to measure them and taking them into account when acquiring terahertz data from time-domain spectroscopy systems.

3. Experimental setup

Our approach to measure the delay deviations is based on interferometrically measuring the time delay in a terahertz time-domain spectroscopy system parallel to the main data acquisition. The first version of the experimental setup of the proposed method is shown in Fig. 4. A standard terahertz time-domain spectroscopy setup driven by a titanium-sapphire laser is used and upgraded with a helium-neon laser fed Mach-Zehnder interferometer. These two subsystems are described in the following subsections.

3.1. Terahertz time-domain spectroscopy system

The terahertz time-domain spectroscopy system is pumped by a passively modelocked titanium-sapphire laser (Coherent© Micra-5™). This laser provides about 200 mW average optical power at a repetition rate of 80 MHz and pulse durations of about 65 fs. As many dispersive optical elements are used in the setup, a pulse compressor prechirps the optical pulses to obtain an optimal pulse duration at the terahertz emitter and detector. In the emitter branch of the time-domain spectroscopy system, a delay-line section is included, containing multiple delay units which are independently investigated in the experimental phase (described in subsection 3.3). The photoconductive switches (Menlo Systems TERA8-1) used as terahertz emitter and detector are pumped with an average optical power of 20 mW each (dipole lengths of 20 μm). The emit-

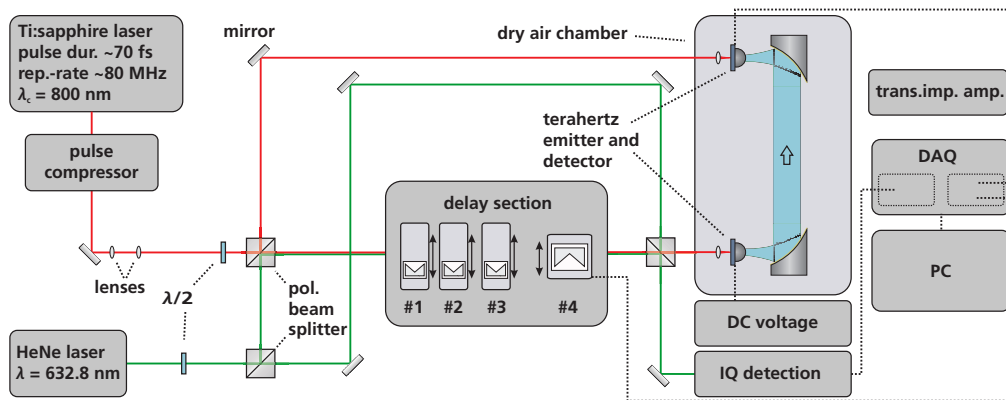


Fig. 4. Experimental setup. A helium-neon laser driven Mach-Zehnder interferometer (green beam path) is integrated into a Ti:Sapphire laser pumped (red beam path) terahertz time-domain spectroscopy system. Both systems share one delay section, in which several different delay lines can be investigated without changing adjustment. This section is only schematically depicted and will be described in more detail in subsection 3.3.

ter antenna is biased with 40 V DC and the detector antenna is connected to a transimpedance amplifier at 10^7 V/A and 200 kHz bandwidth. A data acquisition card with 200 kS per second is used for acquiring the terahertz and interferometer signals simultaneously.

3.2. Interferometer

The integrated Mach-Zehnder interferometer is pumped by a standard helium-neon laser with 1 mW average output power. The coherence length of this source is determined to be longer than 10 cm, which is enough for standard time-domain spectroscopy measuring a maximum delay of a few hundred picoseconds. Polarizing beam-splitter cubes are used to split the output of the laser into the two interferometer branches and to overlap one branch of the interferometer with one branch of the time-domain spectroscopy system perfectly collinear. The delay section therefore is located in the interferometer as well as the time-domain spectroscopy system. After the delay section, the 632.8 nm beam (feeding the interferometer) is separated from the 800 nm beam (driving the time-domain spectroscopy system) by another polarization beam splitter and at the same time overlapped with the reference beam of the interferometer. As the overlapped interferometer beams have different polarization, they do not directly interfere and keep open the possibility to apply an IQ-detection scheme [18, 19]. IQ-detection enables direction detection of movements of the delay, essential for using this principle with highly inaccurate delay units. The output signals of the IQ-detection are connected to counter inputs of the data acquisition, which are synchronized with the input channel of the terahertz detection unit and are acquired at a rate of 200 kHz. The counter is driven in X4-decoding configuration, which provides a time base resolution of 0.53 fs. This high resolution is expected to be also sufficient when using high-bandwidth terahertz time-domain spectroscopy systems in the range of 5 to 30 THz (e.g. air-photonics based systems).

3.3. Delay section

As this experimental setup is built to test and investigate a variety of linear axes and voice-coil driven delay lines, several of them are integrated in series into the delay arm of the time-domain spectroscopy and interferometer setup. This ensures the comparability between the results of different units, as no realignment is necessary when switching between the units. The general scheme of this section is shown in Fig. 5 with sketches of two different spindles used in the

experiments with linear stages. The leadscrew version is in general a low-cost solution to drive

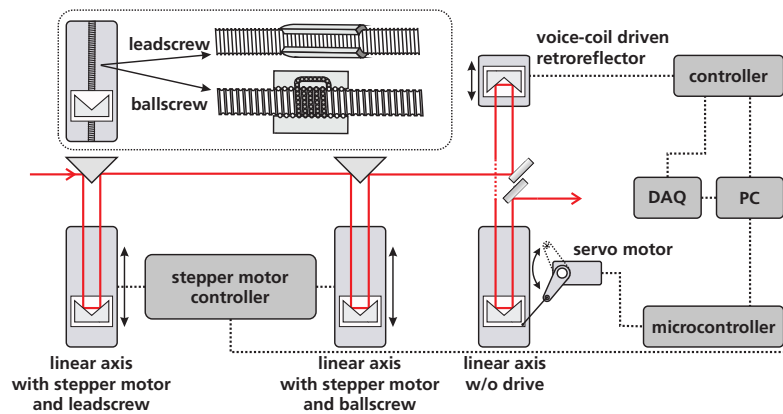


Fig. 5. Delay section of the experimental setup. To evaluate the influence of different delay units, several of them were set up in series. Two stepper-motor controlled linear axes with different spindles (leadscrew and ballscrew version), one linear axis with an attached servo motor (Graupner HBS860MG) as well as a voice-coil driven device were used in the experiments.

linear axes, whereas the circulating ballscrew promises high precision and a uniform movement. The axes in our experiment provide a scan range of several hundred picoseconds and are capable of scanning at velocities up to 20 ps per second. The voice-coil driven delay unit used in this work is a commercially available delay line, which is capable of scanning a delay up to 50 ps or 100 ps (when using double-pass configuration) at frequencies up to 25 Hz. It provides a voltage proportional to the mirror position, derived from an internal position sensitive detector. This signal is usually used as the time base in conventional terahertz time-domain spectroscopy systems employing this delay unit. To prove the applicability of our proposed method, we also combined a servo motor (Graupner HBS860MG) usually used in RC models with a linear guide. This unit represents the most inaccurate delay unit in our setup, as it does not provide any position sensor and shows a highly nonlinear velocity profile.

4. Results

4.1. Influence of delay-line uncertainties on terahertz spectra (experimental)

As mentioned above, we employ different types of delay lines in our terahertz time-domain spectroscopy system, which are characterized in the following. The main parameter to characterize linear stages is their velocity, which determines the measurement duration for the acquisition of a terahertz spectrum at a given resolution. For that reason, we investigate the deviation from a linear translation at different velocities. The result for two different linear stage types is shown in Fig. 6.

For both types, clear resonances can be found, whereas the ballscrew-type linear stage shows significantly less deviation during movement. The leadscrew-type linear stage exceeds a deviation of a few hundred femtoseconds, which is then relevant to the result of pump-probe experiments. Clear resonances and higher harmonics of them can be found, which presumably originate from the stimulation of vibrations of optical components, which were the same on both linear axes. As expected, the ballscrew-type linear stage shows a superior behavior in comparison to the leadscrew-based axis, but also shows clear resonances. The influence of these delay deviations onto the acquired terahertz spectrum when using these types of linear axis is shown in Fig. 7. As expected from theory, symmetric ghost spectra build up at higher frequencies. In

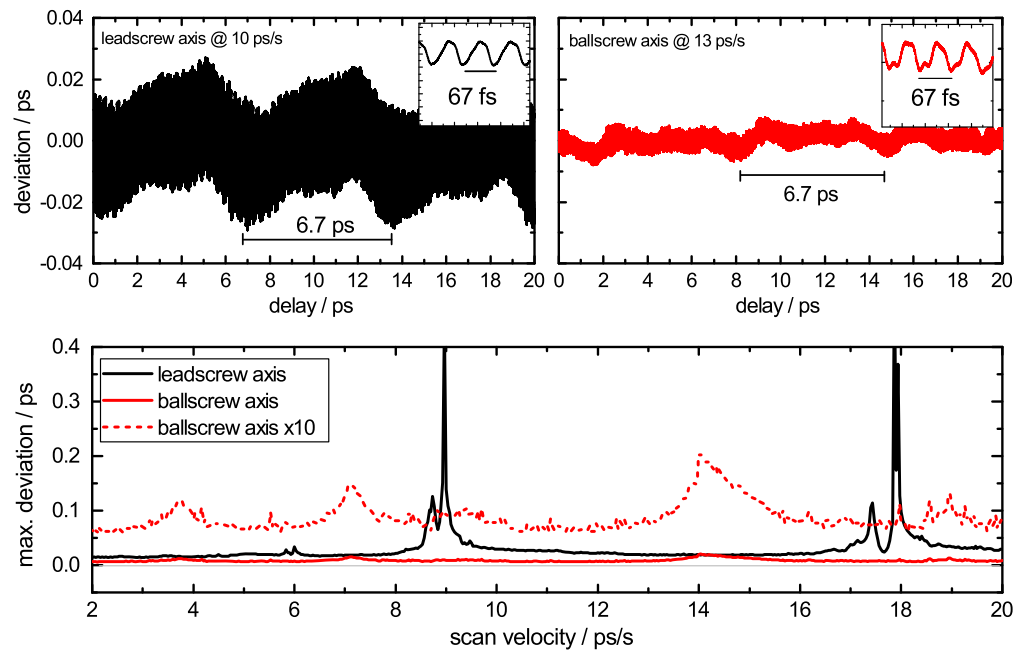


Fig. 6. Delay deviation in dependence on velocity for two different delay lines based on two types of linear stages. Even though both have characteristic resonances, the leadscrew axis shows orders of magnitude higher deviations. The periodicity of 6.7 ps corresponds to the spindle pitch of 1 mm in both cases.

all cases, the center frequency of these ghost spectra is located at 15 THz, corresponding to a delay deviation periodicity of 67 fs. This cannot be fully explained by the spindle pitch of 1 mm, as it leads to a 100 fold periodicity of 6.7 ps. The stepper motor resolution in this case is 400 full steps per revolution, which also does not fit to the factor of 100. We assume mechanical circumstances (e.g. during production of the spindles) to cause this periodicity. The measured time span in these measurements is 200 ps.

The characterization of the voice-coil based device is shown in Fig. 8. Its deviation is obtained by the difference of the position information of the internal sensor and the position information obtained from the interferometer. This difference is measured for different oscillation frequencies and also shows specific resonances. The deviation for the forward and backward scan direction for three oscillation frequencies is shown in the upper plot. Despite the fact, that around the center position, the slope is close to zero and increases towards the reversal point, a clear hysteresis can be found. We acquire the deviation span (maximum to minimum deviation of one cycle) for all oscillation frequencies to find the resonances of the device. The result is shown in the lower plot of Fig. 8. In the vicinity of these resonances, the device behaves very unstable and therefore reacts very sensitive to external disturbances. Because the deviation behavior is not constant or linear with oscillation frequency, no simple scaling factor can be used to correct this error.

4.2. Compensation of systematic delay deviations ("lookup table")

As the systematic deviation of the voice-coil based delay line is constant (from cycle to cycle) when no external disturbance is present, the information from the interferometric characterization can be used to build a so-called lookup-table solution to improve the spectral quality of terahertz time-domain data. This can be done without the integration of an interferometer to the

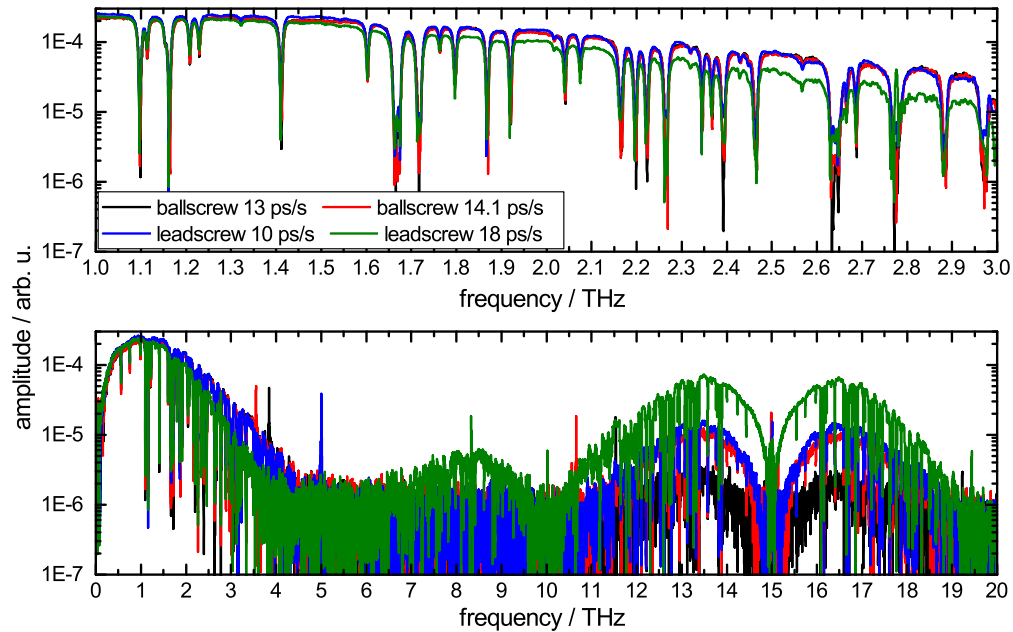


Fig. 7. Terahertz spectra acquired with the two types of linear axes at different scan velocities. In general, the ballscrew version leads to a better quality of the spectrum, which can be seen in a less pronounced ghost spectrum and a better line shape. Corresponding to Fig. 6 and as expected from theory, the ghost spectrum is stronger when scanning on a resonance of the deviation characteristic. For the leadscrew type, the spectrum scanned at a resonance speed of 18 ps/s shows the most impact.

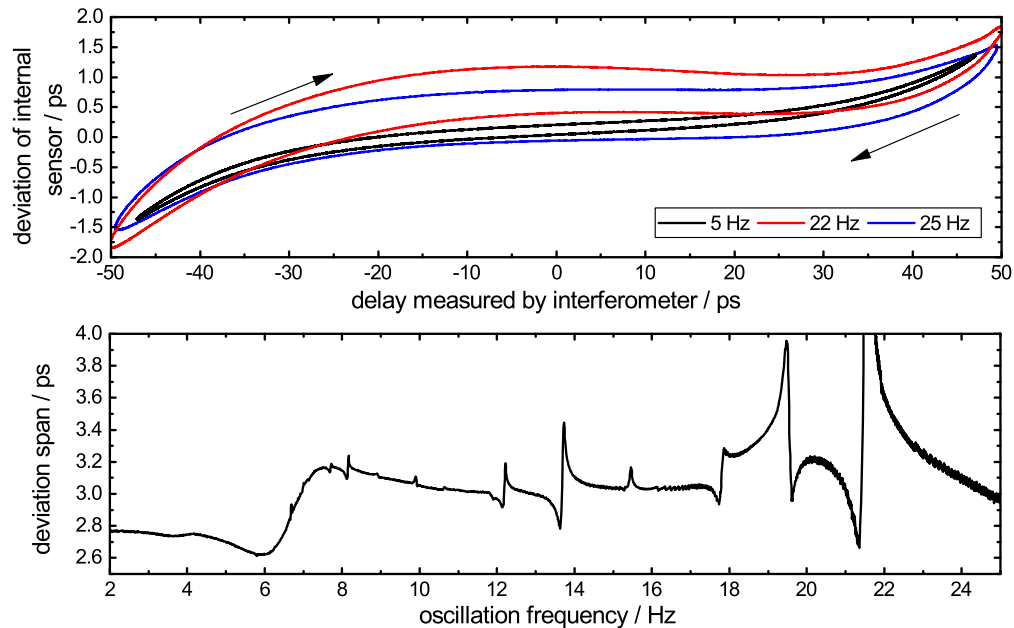


Fig. 8. Delay deviation and deviation span of a voice-coil driven delay line. The internal sensor shows a delay deviation, which is dependent on scan direction, amplitude and frequency. In the upper plot, three examples are shown for maximum amplitude and different frequencies. The deviation span is shown in the lower plot and reveals several resonances.

terahertz time-domain system. For this purpose, we record the mean delay deviation for each setting of the device (2,000 individual measurement sets in total) and save this information on the system. During operation, we monitor the setting of the delay and correct the information of the internal sensor with the data of this lookup table. No simultaneous operation of the interferometer is required here. An example of the signal quality improvement can be seen in Fig. 9, where the spectrum is shown with and without this correction. The improvement is obvious, but is not resistant to external, non-systematic influences. In this experiment the voice-coil driven delay line was used in single-pass configuration, providing a time span of 50 ps. This was taken into account in the presented simulation for comparison.

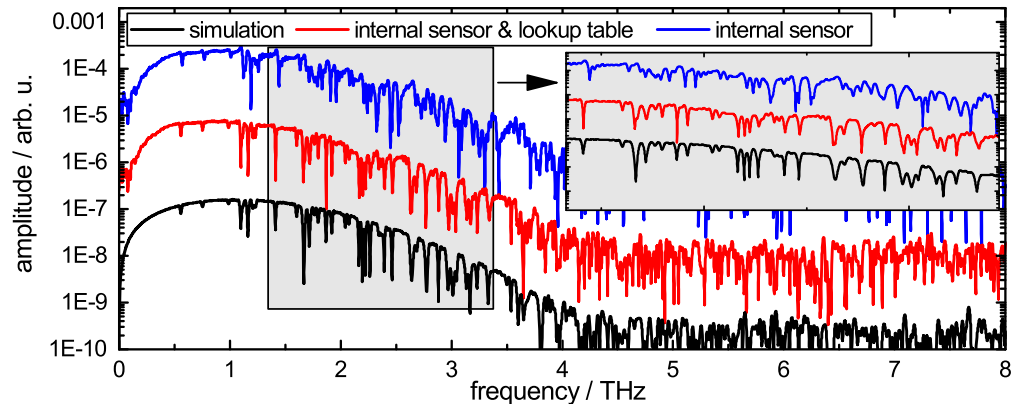


Fig. 9. Improvement in spectral quality when using the lookup-table method. Correction traces are recorded in advance in a separate interferometry setup and transferred onto the time-domain spectroscopy system, in which the delay unit was integrated. Systematic errors can be corrected with this method. Spectra are vertically shifted for clarity.

4.3. Interferometry-aided terahertz time-domain spectroscopy (ITDS) - compensation of systematic and statistic delay deviations

To be fully independent on position sensors of the delay device, we realize the simultaneous operation of the interferometer and the terahertz time-domain spectroscopy system. To demonstrate the potential of this approach we implement a very imprecise servo motor drive (Graupner HBS860MG) in the delay unit without any position feedback during movement. The only feedback is then provided by the interferometer signal. The obtained spectrum is compared to a vertically shifted simulated spectrum in Fig. 10 and proves the applicability of the proposed method. The absorption features from water vapor are accurately measured up to 5 THz with this simple delay unit. In this case the time span is 200 ps for experiment and simulation.

As mentioned above, the lookup-table solution is not able to account for external disturbance. This is also solved when simultaneously operating the interferometer and time-domain spectroscopy system and is of high importance when measuring in real-world industrial environment. To prove the system's immunity to external disturbances when employing the proposed method, we implement this principle to a fiber-coupled terahertz time-domain spectroscopy system, placed on a table. The system based on an ultrafast fiber laser with a center wavelength of 1.55 μm is fully fiber-coupled, except a section in the delay line. During the measurement of terahertz spectra (40 individual spectra per second) of ambient air and evaluation of the center frequency of the 1.41 THz water vapor absorption line, we disturb the system by dropping a 500 g steel ball onto the table several times. The result is shown in Fig. 11 for conventional operation (using the internal position sensor of the voice-coil driven delay unit) and for the interferometry-aided operation. While the deviation in the conventional case exceeds 10 GHz

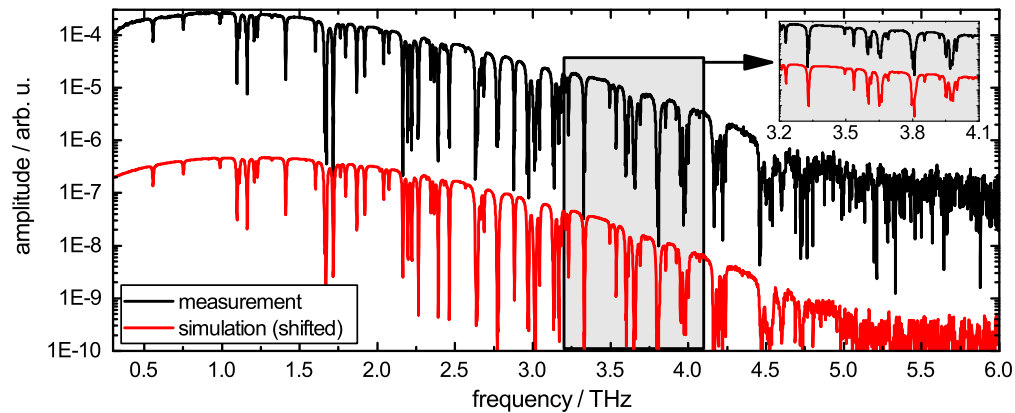


Fig. 10. Terahertz spectrum measured with a servo motor driven delay unit using the interferometry-aided terahertz time-domain spectroscopy method in comparison to a simulated spectrum (shifted vertically). Even though, the servo motor provides no position feedback, nor a constant velocity during movement, the absorption features are measured well up to 5 THz. The scanned time-domain span was 200 ps and the acquisition time was about 10 s.

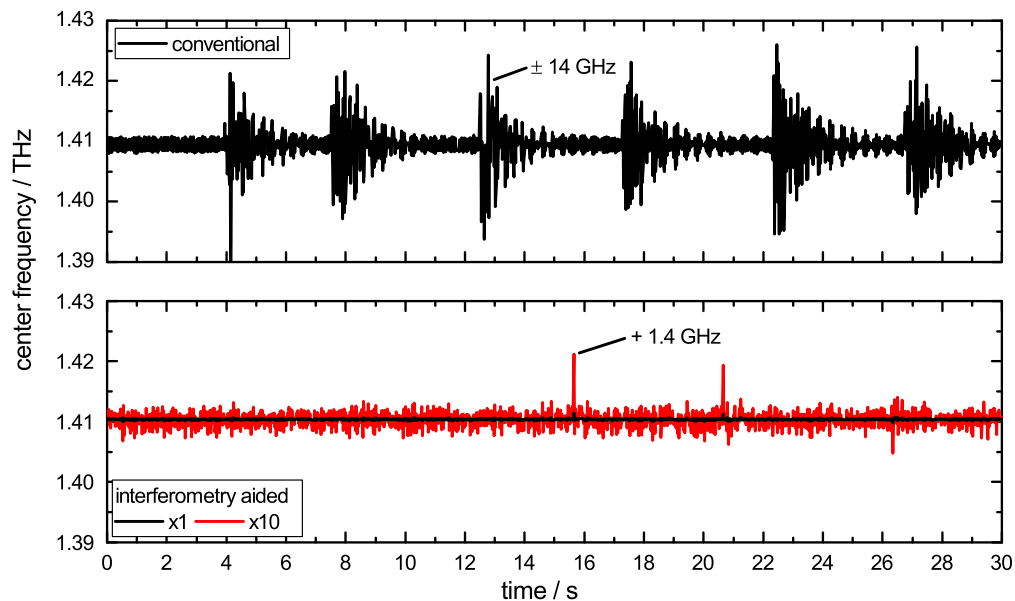


Fig. 11. Comparison of the influence of mechanical shock onto a fiber-coupled terahertz time-domain spectroscopy system without and with interferometrically aided delay lines. For evaluation, the 1.41 THz water vapor absorption line was analyzed for its center frequency continuously. The shock was induced by dropping a 500 g steel ball onto the table, the system was placed on. Without interferometer (conventional method), strong deviations greater than 10 GHz occur, whose decay time is more than a second. With interferometrically tracked delay line, the system shows almost no deviation (within the shown time window, the steel ball was also dropped six times). Small deviations up to 1.4 GHz occur, but decay very fast.

and shows strong oscillatory and decaying behavior, the interferometry-aided case barely shows any influence. Only singular events show a deviation of about 1.4 GHz for the position of the absorption line. Due to the fast decay of this small deviation, we assume the origin of this to be located somewhere outside the interferometer. This clearly demonstrates the improvement in signal stability when employing our proposed method. When evaluating the time delay of the terahertz signal maximum at a scan rate of 40 Hz during one minute we achieve a standard deviation of about 2 fs. This stability is important when averaging successive time traces without losing spectral resolution.

5. Summary

We have presented a comprehensive study of the influence of delay deviation errors for linear-axis-based delay lines as well as voice-coil driven delay units. By implementing a Mach-Zehnder interferometer into a terahertz time-domain spectroscopy system, we achieve an exact timing information for the evaluation of acquired terahertz pulses. The coaxial overlap of the interferometer beam with one of the pump beams of the time-domain spectroscopy system ensures the highest accuracy of the time stamps. Our proposed method improves the stability and accuracy of terahertz time-domain spectroscopy systems and lowers the need for mechanically and electronically stable translation stages used for optical delay lines.

Funding

This work was supported by the Fraunhofer Internal Program MEF under Grant No. 83 05 34.

Acknowledgments

We acknowledge the support of our colleagues at the Fraunhofer Institute for Physical Measurement Techniques IPM, Freiburg, Germany.